

Structure and Bonding Properties of the Complex (η^5 -Diphenylfulvene)Mn(CO) $_3^+$

Martin A. O. Volland, Steffen Kudis, Günter Helmchen,* Isabella Hyla-Kryspin,
Frank Rominger, and Rolf Gleiter*

Organisch-Chemisches Institut der Universität Heidelberg, Im Neuenheimer Feld 270,
D 69120 Heidelberg, Germany

Received July 10, 2000

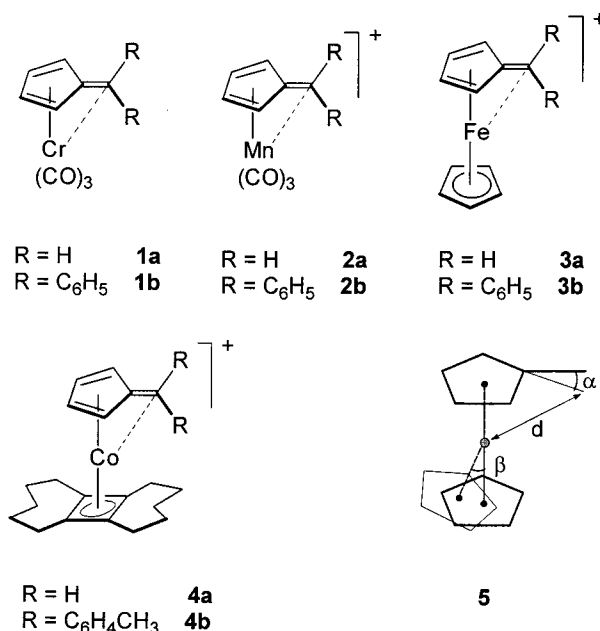
Summary: Reaction of cymantrene (**6**) with *n*-butyllithium followed by benzophenone and subsequent hydrolysis yielded 1-(diphenylhydroxymethyl)(η^5 -cyclopentadienyl)(tricarbonyl)manganese (**7**). Treatment of **7** with HBARF·2Et $_2$ O in methylene chloride affords the blue cation **2b**. Investigations of single crystals of **2b** by means of the X-ray technique showed a displacement of the exo carbon by 6.6° toward the metal and a pronounced bond alternation of the C–C bonds of the fulvene moiety. DFT calculations on the parent system **2a** and on a system with a planar fulvene moiety (**2a'**) yielded an energy difference of 23 kJ/mol in favor of **2a**. As a result of the bending of the exo methylene group the positive charge at the metal is increased and at C9 decreased.

Introduction

In the series of fulvene complexes¹ with transition metals of groups VI–VIII, the structures of **1b**,² **3b**,³ and **4b**⁴ have been investigated by means of the X-ray technique. Common to all of them is a bending of the diphenylmethylidene group toward the metal expressed by the parameters α and d as shown in **5**. It is most pronounced in the case of **1b** ($\alpha = 31^\circ$)² and less in **4b** ($\alpha = 11^\circ$ or 6°).⁴ In this series data on **2** are missing. Therefore we have synthesized **2b** and investigated the structure by applying the X-ray technique. In addition to these experimental investigations we have carried out model calculations on **2a** by using the density functional theory (DFT).⁵

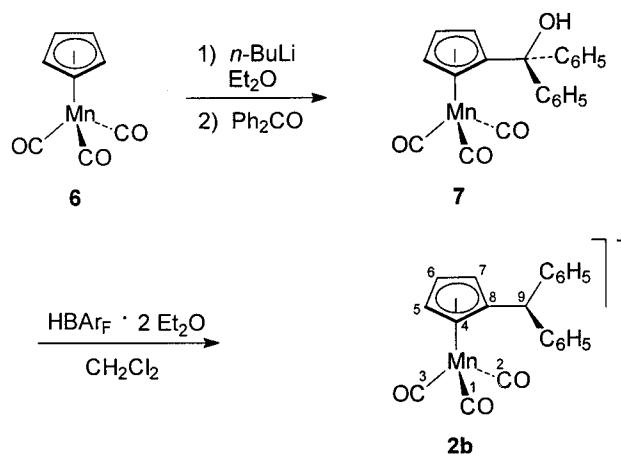
Results and Discussion

The preparation of **2b** commenced with cymantrene **6** which was metalated at -78°C with *n*-BuLi. The lithio derivative was treated with benzophenone to give the alcohol **7** in 87% yield (Scheme 1). Treatment of a solution of the alcohol in dichloromethane with an



equimolar amount of the bis(ether) complex of tetrakis-[3,5-bis(trifluoromethyl)phenyl]boric acid (HBArF·2Et $_2$ O)⁶ furnished a deep blue solution from which **2b** can be isolated in 60% yield as the BA r F $^-$ salt. Single crystals obtained from a CH $_2$ Cl $_2$ /pentane solution of **2b**BA r F $^-$ at -6°C allowed a high quality X-ray crystal structure analysis to be carried out. The molecular structures of **2b** and **7** are displayed in Figure 1. The most relevant distances of both structures are listed in Table 1. As anticipated from the isolobal species **1b** we find in **2b** a

Scheme 1



(1) For reviews, see: Kerber, R. C.; Ehntholt, D. J. *Synthesis* **1970**, 449. Watts, W. E. *Organomet. Chem. Rev.* **1979**, 7, 399. Cais, M. *Organomet. Chem. Rev.* **1966**, 1, 435.

(2) Andrianov, V. G.; Struchkov, Y. T.; Setkina, V. N.; Zdanovich, V. I.; Zhakaeva, A. Z.; Kursanov, D. N. *J. Chem. Soc. Chem. Commun.* **1975**, 117.

(3) Behrens, U. *J. Organomet. Chem.* **1979**, 182, 89.

(4) Gleiter, R.; Schimanke, H.; Silverio, S. J.; Büchner, M.; Huttner, G. *Organometallics* **1996**, 15, 5635.

(5) Parr, R. G.; Yang, W. *Density-Functional Theory of Atoms and Molecules*; Oxford University Press: Oxford, 1989. Koch, W.; Holthausen, M. C. *A Chemist's Guide to Density Functional Theory*; Wiley-VCH: Weinheim, 2000.

(6) Brookhart, M.; Grant, B.; Volpe, A. F., Jr. *Organometallics* **1992**, 11, 3920.

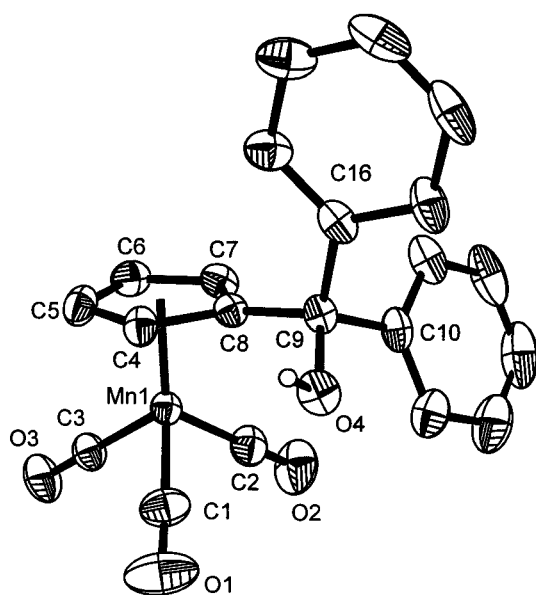
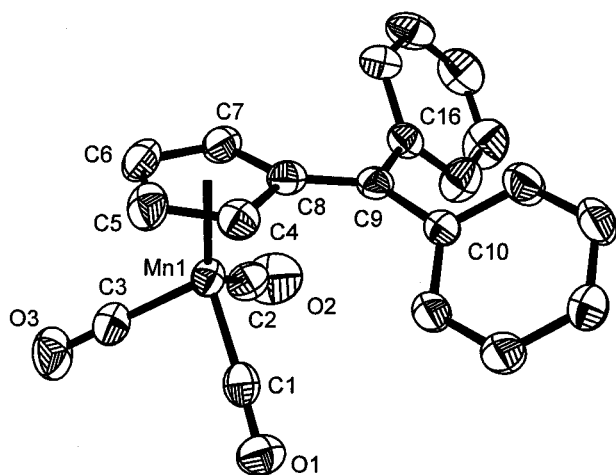


Figure 1. ORTEP drawing of **2b** (top) and **7**. The core atoms are labeled. Ellipsoids are at the 50% probability level. The hydrogen atoms except for H4 have been omitted for the sake of clarity.

Table 1. Selected Interatomic Distances (Å) for **2b** and **7**

Compound 2b			
Mn–C1	1.812(5)	C1–O1	1.142(5)
Mn–C4	2.134(4)	C4–C5	1.393(6)
Mn–C5	2.167(4)	C5–C6	1.415(6)
Mn–C6	2.156(4)	C6–C7	1.389(6)
Mn–C7	2.115(4)	C4–C8	1.452(6)
Mn–C8	2.131(4)	C7–C8	1.456(5)
Mn–C9	3.045(5)	C8–C9	1.413(5)
Compound 7			
Mn–C1	1.797(2)	C1–O1	1.142(2)
Mn–C4	2.140(2)	C4–C5	1.414(2)
Mn–C5	2.143(2)	C5–C6	1.419(3)
Mn–C6	2.144(2)	C6–C7	1.414(2)
Mn–C8	2.150(2)	C7–C8	1.413(2)
Mn–C9	3.340(2)	C8–C9	1.518(2)

bending of the C8–C9 bond by $\alpha = 7^\circ$ (as defined in **5**) toward the metal. We notice also a bond alternation in the fulvene ring. The bonds C4–C5 and C6–C7 are shorter (1.39 Å) than C5–C6 (1.42 Å) and C4–C8 or C7–C8 (1.45 Å). This alternation of the carbon bonds is not found in the five-membered ring of **7** (Table 1).

Table 2. Selected Geometrical Parameters for **1b–4b**

compd	α (deg)	β (deg)	d (Å)	ref
1b	31.0		2.53	2
2b	6.6		3.05	this work
3b	20.7	8.1	2.72	3
4b^a	10.8	12.4	2.95	4
4b^a	6.4	13.4	3.03	4

^a There are two independent molecules in the unit cell.

In Table 2 we have compared the parameters α , β , and d (as defined in **5**) for **1b–4b**. In all four cases there is an interaction between the exo carbon and the metal. It is smallest in **2b** and **4b** and largest in **1b**. The interaction prevailing in **2b** can also be seen from the comparison between the ^{13}C NMR spectra of **2b** with **7**. The difference in the ^{13}C chemical shift of the exo-methylidene carbon was found to be $\Delta\delta$ (**7–2b**) 91.4 ppm. The corresponding values for **3b**⁴ and **4b**⁴ are 71 and 65 ppm, respectively.

To understand the electronic effects we optimized the geometry of **2a** fully within C_s symmetry constraints. All calculations were carried out with the hybrid Hartree–Fock/density functional theory method, known by its acronym B3LYP.⁷ A single all-electron basis set was used throughout the present studies. The Mn atom was described by Wachters (14s, 9p, 5d) basis set⁸ augmented with a 4f polarization function ($\alpha_f = 0.96$). The contraction scheme of [9s, 5p, 3d, 1f] corresponds to a double- and triple- ξ basis for the core and valence electrons, respectively. Standard 6-311G* basis sets were used for C, O, and H.⁹ The presented structures were optimized with analytical gradient procedures and correspond to fully converged geometries with gradients and displacements below the standard thresholds. To test the stationarity of the optimized structures, vibrational frequencies were obtained from analytical calculations of the Hessian matrixes. The electronic structure of the investigated compounds was characterized with help of the natural population analysis (NPA) and natural bond orbital (NBO) methods.¹⁰ The calculations have been carried out with the Gaussian 98 program¹¹ installed on the IBM RS/6000 workstations of our laboratory and of the Universitätsrechenzentrum Heidelberg. For graphical displays we used the Molek-9000¹² and GaussView¹³ programs.

(7) Becke, A. D. *J. Chem. Phys.* **1992**, *96*, 2155; *J. Chem. Phys.* **1993**, *98*, 5648. Vosko, S. H.; Wilk, L.; Nusair, M. *Can. J. Phys.* **1980**, *58*, 1200. Lee, C.; Yang, W.; Parr, R. G. *Phys. Rev. B* **1988**, *37*, 785.

(8) Wachters, A. J. H. *J. Chem. Phys.* **1970**, *52*, 1033.

(9) Krishnan, R.; Binkley, J. S.; Seeger, R.; Pople, J. A. *J. Chem. Phys.* **1980**, *72*, 650.

(10) Foster, J. P.; Weinhold, F. *J. Am. Chem. Soc.* **1980**, *102*, 7211. Reed, A. E.; Weinhold, F. *J. Chem. Phys.* **1983**, *78*, 4066. Reed, A. E.; Weinstock, R. B.; Weinhold, F. *J. Chem. Phys.* **1985**, *83*, 735. Reed, A. E.; Curtiss, L. A.; Weinhold, F. *Chem. Rev.* **1988**, *88*, 899.

(11) Gaussian 98, Revision A.5. Frisch, M. J.; Trucks, G. W.; Schlegel, H. B.; Scuseria, G. E.; Robb, M. A.; Cheeseman, J. R.; Zakrzewski, V. G.; Montgomery, J. A., Jr.; Stratmann, R. E.; Burant, J. C.; Dapprich, S.; Millam, J. M.; Daniels, A. D.; Kudin, K. N.; Strain, M. C.; Farkas, O.; Tomasi, J.; Barone, V.; Cossi, M.; Cammi, R.; Mennucci, B.; Pomelli, C.; Adamo, C.; Clifford, S.; Ochterski, J.; Petersson, G. A.; Ayala, P. Y.; Cui, Q.; Morokuma, K.; Malick, D. K.; Rabuck, A. D.; Raghavachari, K.; Foresman, J. B.; Cioslowski, J.; Ortiz, J. V.; Stefanov, B. B.; Liu, G.; Liashenko, A.; Piskorz, P.; Komaromi, I.; Gomperts, R.; Martin, R. L.; Fox, D. J.; Keith, T.; Al-Laham, M. A.; Peng, C. Y.; Nanayakkara, A.; Gonzalez, C.; Challacombe, M.; Gill, P. M. W.; Johnson, B.; Chen, W.; Wong, M. W.; Andres, J. L.; Head-Gordon, M.; Replogle, E. S.; Pople, J. A. Gaussian, Inc.: Pittsburgh, PA, 1998.

Table 3. Selected Distances (Å) Resulting from a DFT Calculation on **2a (C_s)**

Mn–C1	1.858	C1–O1	1.133
Mn–C4	2.157	C4–C5	1.391
Mn–C5	2.232	C5–C6	1.448
Mn–C8	2.052	C8–C9	1.384
Mn–C9	2.429		

Table 3 lists the most relevant distances obtained. These data agree well with the X-ray data (Table 1), except for the angle α . In this case we calculated 31° whereas the experiment yielded only 6.6° . This difference might be attributed to steric effects; however, for **1b** a bending angle of 31° was reported.² It is interesting to note that both extended Hückel¹⁴ and DFT calculations¹⁵ on **3a** predict larger values for α of 40° and 41° , respectively, whereas the diffraction studies yielded 21° for **3b**.³ In the sterically less crowded ruthenocene and osmocene derivatives ($C_5Me_5MC_5Me_4CH_2^+$, M = Ru, Os) the CH_2 group was bent by $\alpha = 40.3^\circ$ and 41.8° , respectively.¹⁶

We also optimized the structure of a species with a planar fulvene complexed to a $Mn(CO)_3$ unit (**2a'**).¹⁵ The main difference of **2a** and **2a'** is an elongation of the

C8–C9 bond. It is calculated to be 1.36 Å in **2a'** and 1.38 Å in **2a**. The energy difference between **2a** and **2a'** was calculated to be 23 kJ/mol. In Figure 2 we present a correlation diagram between the frontier orbitals of **2a'** and **2a**. As a result of the bending of C9 toward the metal the LUMO is strongly destabilized due to the antibonding interaction between the 2p orbital at C9 and the metal 3d orbital. With the exception of $1a''$ four of the highest occupied orbitals are stabilized by the bending (Figure 2). A population analysis yields a slight increase of the positive charge at the metal in **2a** (0.724) as compared to **2a'** (0.716) and at C9 a decrease (0.328 in **2a'** and 0.175 in **2a**).

Experimental Section

Equipment. All melting points are uncorrected. The NMR spectra were measured with a Bruker AS 300 (1H NMR at 300 MHz and ^{13}C NMR at 75.5 MHz) using the solvent (CD_2Cl_2) for calibration ($\delta = 5.31$). High-resolution mass spectra (HRMS) were obtained with a ZAB-3F (Vacuum Generators) and JEOL JMS 700 high-resolution mass spectrometer. The UV/vis spectra were recorded on a Hewlett-Packard HP8452 diode spectrometer. Microanalyses were performed at the

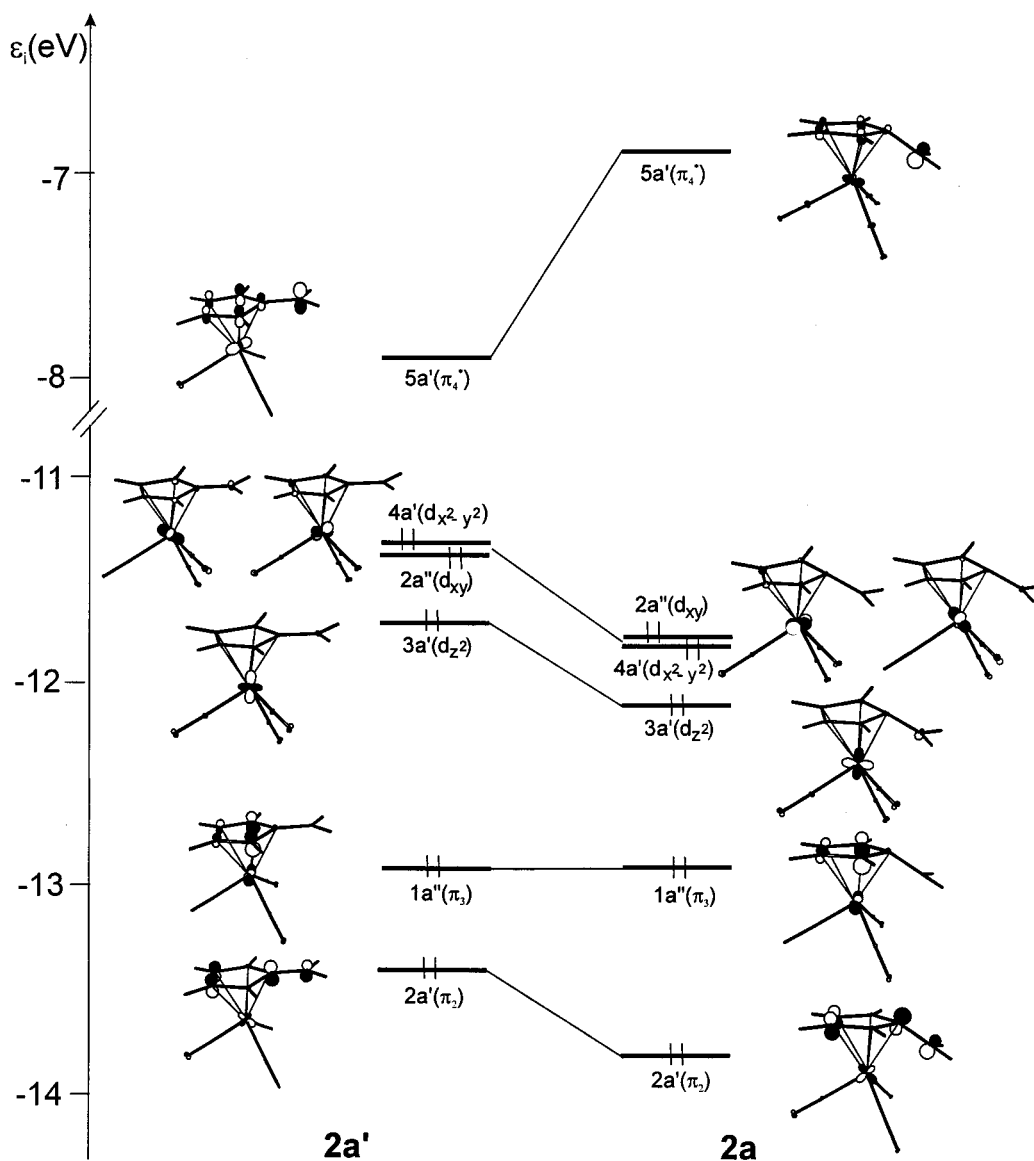


Figure 2. Correlation diagram between the frontier orbitals of a planar **2a'** and a bent cation (**2a**).

Table 4. Crystal Data and Structure Refinement for 2b and 7

	7	2b
emp form	C ₂₁ H ₁₅ MnO ₄	C ₅₄ H ₂₈ BCl ₂ F ₂₄ MnO ₃
form wt	386.3	1317.41
cryst color	yellow	blue
cryst shape	polyhedron	polyhedron
cryst size [mm]	0.36 × 0.30 × 0.28	0.36 × 0.24 × 0.07
T [K]	200	200
wavelength [Å]	0.71073	0.71073
cryst syst	monoclinic	triclinic
space group	C2/c	P1
Z	8	2
a [Å]	19.8003(3)	12.6457(8)
b [Å]	7.0936(1)	14.0369(9)
c [Å]	27.0656(2)	16.614(1)
α [deg]	90.0	75.733(1)
β [deg]	109.317(1)	77.770(1)
γ [deg]	90.0	71.565(1)
V [Å ³]	3587.49(8)	2682.6(3)
D _{calcd} [g/cm ³]	1.43	1.63
abs coeff., μ [mm ⁻¹]	0.76	0.47
θ range [deg]	2.2–27.5	1.6–25.6
index ranges	–25 ≤ h ≤ 25 –9 ≤ k ≤ 9 –35 ≤ l ≤ 35	–14 ≤ h ≤ 15 –17 ≤ k ≤ 16 –20 ≤ l ≤ 19
no. of refls collected	17762	20108
no. of unique refls	4116	8993
max and min transmission	0.86 and 0.75	0.97 and 0.74
no of obsd data/params	3621/236	5767/878
GOF on F ²	1.06	1.01
R (F)	0.031	0.046
R _w (F ²)	0.082	0.098
(Δρ) _{max} , (Δρ) _{min} [eÅ ⁻³]	0.34–0.36	0.48–0.34

Mikroanalytisches Laboratorium der Chemischen Institute der Universität Heidelberg.

(1-(Diphenylhydroxymethyl)cyclopentadienyl)manganese Tricarbonyl (7). To a solution of 2.0 g (9.8 mmol) of cymantrene (**6**) in 25 mL of dry ether was added at –78 °C 6.7 mL (10.8 mmol) of a 1.6 M solution of *n*-BuLi in hexane. After the mixture was stirred at –78 °C for 30 min it was warmed within 30 min to –20 °C. A color change from light yellow to dark brown was observed. Subsequently the mixture was cooled to –50 °C and a solution of 2.0 g (10.8 mmol) of benzophenone in 15 mL of dry ether was added. After the mixture was warmed to 0 °C within 3 h it was hydrolyzed with a saturated solution of NH₄Cl in water. The layers were separated; the organic phase was washed with saturated NaCl solution in water, dried with Na₂SO₄, and concentrated in vacuo. The residue was chromatographed (alumina, petroleum

ether/ether 9:1, *R_f* = 0.26) and yielded 3.27 g (87%) of **7** as a yellow solid. For **7**: mp 122 °C; ¹H NMR δ 2.72 (bs, 1H, OH), 4.69 (bs, 2H, CpH), 4.87 (bs, 2H, CpH), 7.31 (bs, 10H, ArH); ¹³C NMR δ 77.4 (*i*-CpC), 80.5 (CpCH), 87.1 (CpCH), 111.7 (COH), 127.1, 127.7, 128.0 (ArCH), 146.8 (ArC), 224.8 (CO); UV/vis (CH₂Cl₂) (λ_{max}, nm (log ε)) 328 (3.1); HRMS calcd for C₂₁H₁₅MnO₄ *m/z* 386.0351, found *m/z* 386.0362. Anal. Calcd for C₂₁H₁₅MnO₄ (386.0): C, 65.30; H, 3.91. Found: C, 65.27; H, 3.97.

(Tricarbonyl){η⁵-(diphenylum)cyclopentadienyl}manganese Tetrakis[3,5-(trifluoromethyl)phenyl]borate (2bBARF). To a solution of **7** (30 mg, 0.078 mmol) in 2 mL of dry CH₂Cl₂ was added at room temperature 86 mg (0.086 mmol) of [3,5-(CF₃)₂C₉H₃]₄B[–]H(OEt₂)₂⁺ (HBARF·2Et₂O)⁶ under argon (glovebox). The blue solution was stirred for 10 min at room temperature. After reduction of the volume of the solution to 1 mL and addition of 5 mL of pentane, a blue oil separated. The oil was suspended in 5 mL of pentane and vigorously stirred, and then volatiles were removed in vacuo. Repeating this procedure three times led to the formation of a blue powder that was washed three times with 5 mL of pentane. Drying in vacuo yielded 60 mg (60%) of **2bBARF** as a blue microcrystalline solid. For **2bBARF**: mp 102 °C; ¹H NMR δ 5.83 (“t”, *J* = 2.3 Hz, 2H, CpH), 6.11 (“t”, *J* = 2 Hz, CpH), 7.55 (bs, 4H, *p*-Ar_F-H), 7.56 (s, 4H, *o*-Ar_F-H), 7.62 (“t”, *J* = 8.3 Hz, *m*-Ar_F-H), 7.72 (bs, 8H, *o*-Ar_F-H), 7.96 (“t”, *J* = 7.3 Hz, 2H, *p*-Ar_F-H); ¹³C NMR δ 95.8, 96.4 (CpC), 97.0 (*i*-CpC), 117.6 (*p*-Ar_FC), 124.7 (q, ¹*J*_{C–F} = 272 Hz, CF₃), 129.0 (q, ²*J*_{C–F} = 30 Hz, *m*-Ar_F-C), 130.2, 134.4 (*o*- and *m*-Ar_F-C), 134.9 (bs, *o*-Ar_F-C), 138.7 (*i*-ArC), 139.4 (*p*-Ar_F-C), 161.8 (q, ¹*J*_{BC} = 50 Hz, BC), 203.1 (CPh₂), 217.2 (CO); UV/vis (CH₂Cl₂) (λ_{max}, nm (log ε)) 266 (4.0), 390 (4.3), 614 (3.9); HRMS calcd for C₂₁H₁₄MnO₃ *m/z* 369.0323, found 369.0338. Anal. Calcd for C₅₃H₂₆BF₂₄MnO₃: C, 51.65; H, 2.13. Found C, 51.65; H, 2.11.

X-ray Crystallography and Structure Solution. Data were collected on a Bruker SMART CCD diffractometer at 200 K. Relevant crystal and data collection parameters are given in Table 4. The structures of **2b** and **7** were solved by using direct methods, least-squares refinement, and Fourier techniques. Structure solution and refinement were performed with SHELXTL V 5.10.¹⁷

Acknowledgment. We are grateful to the Deutsche Forschungsgemeinschaft (SFB 247), the Fonds der Chemischen Industrie, and the BASF Aktiengesellschaft for financial support. M.A.O.V. acknowledges the Studienstiftung des deutschen Volkes for a fellowship. We thank Mrs. A. Reule for typing the manuscript.

Supporting Information Available: Tables of atomic coordinates and thermal parameters, and bond lengths and angles for **2b** and **7**. This material is available free of charge via the Internet at <http://pubs.acs.org>.

OM000587Q

(12) Bischof, P. *Molek-9000*, Universität Heidelberg, 1998.

(13) *GaussView* Gaussian, Inc.: Pittsburgh, PA, 1998.

(14) Gleiter, R.; Seeger, R. *Helv. Chim. Acta* **1971**, *54*, 1217.

(15) Hyla-Kryspin, I.; Gleiter, R. Unpublished results.

(16) Rybinskaya, M. I.; Kreindlin, A. Z.; Struchkov, Y. T.; Yanovsky, A. I. *J. Organomet. Chem.* **1989**, *359*, 233; Yanovsky, A. I.; Struchkov, Y. T.; Kreindlin, A. Z.; Rybinskaya, M. I. *J. Organomet. Chem.* **1989**, *369*, 125.

(17) Sheldrick, G. M. *SHELXTL V 5.10*, Bruker Analytical X-ray Division: Madison, WI, 1997.